

Crack velocity measurement by induced electromagnetic radiation

V. Frid^{a,*}, A. Rabinovitch^b, D. Bahat^a

^a *The Deichmann Rock Mechanics Laboratory of the Negev, Geological and Environmental Sciences Department, Ben Gurion University of the Negev, Beer Sheva, Israel*

^b *The Deichmann Rock Mechanics Laboratory of the Negev, Physics Department, Ben Gurion University of the Negev, Beer Sheva, Israel*

Received 11 December 2005; received in revised form 10 March 2006; accepted 10 March 2006

Available online 22 March 2006

Communicated by R. Wu

Abstract

Our model of electromagnetic radiation (EMR) emanated from fracture implies that EMR amplitude is proportional to crack velocity. Soda lime glass samples were tested under uniaxial tension. Comparison of crack velocity observed by Wallner line analysis and the peak amplitude of EMR signals registered during the test, showed very good correlation, validating this proportionality.

© 2006 Elsevier B.V. All rights reserved.

PACS: 81.70.-q; 61.80.-x; 62.20.Mk

Keywords: Crack velocity; Fracture; Electromagnetic radiation

1. Introduction

Electromagnetic radiation (EMR) emanating from fracture is an extensively investigated phenomena, e.g., [1–3]. The correlation between crack sizes and pulse parameters were carefully verified [4–6]. Our EMR model [6,7] predicts (see below) that crack velocity should be proportional to the EMR amplitude. However no actual proof of EMR use for crack velocity evaluation has hitherto been provided. Here we compare crack velocity evaluations by both Wallner line analysis and EMR, and demonstrate that EMR amplitude can indeed be used for quantitative analysis of crack velocity changes.

Note that other methods to measure crack velocity are known, e.g., changes of electrical conductivity. These methods require either special preparation of the sample surfaces or be used only for transparent materials. These limitations could be avoided by using EMR as the measuring mechanism.

2. Brief theoretical considerations

We describe briefly the aspects of both EMR and Wallner lines which are relevant for our analysis.

2.1. EMR

A model to explain EMR emitted by fracture was developed by our group [6,7] and is briefly presented here. In this model it is assumed that, following the breaking of bonds by the moving fracture, the atoms on both created sides are moved to “nonequilibrium” positions relative to their steady state ones and oscillate around them. Lines of oscillating atoms move together and, being connected to atoms around them (both in the forward direction and on their side), the latter also participate in the movement. The ensuing vibrations are surface vibrational waves: positive charges move together in a diametrically opposite phase to the negative ones while decaying exponentially into the material, like Rayleigh waves. The resulting oscillating electric dipoles act as the source of the EMR. The wave’s amplitude decays by an interaction with bulk phonons.

In this model [6,7], the shape of an individual EMR pulse has the form [4] given by

* Corresponding author.
E-mail address: vfrid@bgu.ac.il (V. Frid).

$$A(t) = \begin{cases} A_0[1 - e^{(-\frac{t}{\tau})}]f(\omega t), & 0 < t < T, \\ A_0[1 - e^{(-\frac{T}{\tau})}]e^{(-\frac{t-T}{\tau})}f(\omega(t-T)), & t > T. \end{cases} \quad (1)$$

Here A_0 is the maximum amplitude of the pulse, and T is the time when the amplitude reaches its maximum value, f is an oscillating function; ω is the pulse frequency and τ is the rise and fall times (which turn out to be the same). The model implies that T is proportional to crack length [4], the pulse frequency ω is inversely proportional to the crack width [8] and the maximum amplitude is given by

$$A_0 = \alpha v_{\text{cr}} \tau, \quad (2)$$

where v_{cr} is the crack velocity. This relation is true provided v_{cr} remains constant during the short interval T , which we assume throughout.

α can be described by the following relationship:

$$\alpha = BG \int f(\Omega) d\Omega q(\omega) d(\omega), \quad (3)$$

where B is the power of the EMR, a part of the entire power of fracturing, G is the gain factor, $f(\Omega) d\Omega$ characterizes the polarization of EMR as a function of the solid angle Ω and $q(\omega)$ represents the antenna frequency response in volts/(watt herz).

Since τ was shown to be inversely proportional to the EMR signal frequency ω [8], it is a constant for signals of the same frequency. Moreover, for short cracks (less than 1 mm in length) it can be assumed that crack length is proportional to crack width and hence T too is inversely proportional to crack frequency ω . It means that for cracks inducing short EMR signals of the same frequency, both T and τ will be constant implying that the maximal EMR amplitude will actually be proportional to v_{cr} .

It can be shown [9] that if two pulses overlap, and the initiation time difference between them (t_0) is larger than the time to reach maximum amplitude of the first one (T_1), Eq. (2) can still be used.

We assume that

- (a) The number of closely overlapping pulses (i.e., $t_0 < T_1$) is vanishingly small so that Eq. (1) can be applied throughout.
- (b) Velocity changes during the time interval T are negligible.

2.2. Wallner lines

Wallner lines, named after the scientist who first explained them [10–12] constitute a unique “post mortem” tool for evaluating crack velocity in brittle materials [12–14]. These lines are delicate traces observed on fracture surfaces of brittle materials produced by the interaction of the crack front and transverse acoustic waves generated either naturally by discontinuities such as sample edges or artificially by a transducer [15,16]. The contour of the Wallner lines depends on the ratio of the crack speed v_{cr} and the speed of the transverse stress waves, c_s . There exist in the literature three geometrical methods [17] for Wallner line analysis. For the implementation of which a precise knowledge of at least two important data are needed: either (1) the crack nucleation position (and/or crack propagation direction) and (2) the point of origin of at least one Wallner line;

or, alternatively, the points of origin of two Wallner lines. The locations of the point of crack nucleation and of the origin of the Wallner line are usually known only imprecisely, especially when the crack propagates in an intensive manner. As a result and due to the relatively large errors incurred in measuring angles, crack velocities obtained by Wallner lines analysis are often grossly inaccurate or even unobtainable.

We have developed a novel method of Wallner lines analysis, based on first principles, which can rectify these problems [18], and in the process of which in addition to the evaluation of the crack velocity magnitude, the points of origin of both the crack and the Wallner line are obtained, as well as the velocity by which the information about the fracture initiation traveled from the latter’s origin up to the origin of the Wallner line [18].

The method is based on the following simple approach. The interaction, at time t , of the crack front and the acoustic wave, propagating from A (at time $t = 0$) and from B (at time t_1 when information reached it), respectively is given by

$$(x - a)^2 + (y - b)^2 = v_{\text{cr}}^2 t^2, \quad (4)$$

$$(x - c)^2 + (y - d)^2 = c_s^2 (t - t_1)^2, \quad (5)$$

where x and y are the current coordinates of the Wallner line point; A (a, b) is the crack initiation point; B (c, d) is the origin of the acoustic wave; v_{cr} is the crack velocity and c_s is the transverse wave speed. Eliminating t from Eqs. (4) and (5) leads to Eq. (6), an implicit relation describing the Wallner line contour $y(x)$ through

$$z \equiv (x - c)^2 + (y - d)^2 - w(\sqrt{(x - a)^2 + (y - b)^2} - s)^2 = 0, \quad (6)$$

where $w (= 1/u^2) = c_s^2/v_{\text{cr}}^2$ and $s = v_{\text{cr}}t_1$ is the distance the crack propagates in the time interval t_1 . Eq. (6) is used together with measured points across the Wallner line to extract the unknown parameters a, b, c, d, s and w by a least square method.

We conducted our numeral experiments by using the Nonlinear-Fit package of “Mathematica” that enabled us to fit the six parameters of the implicit function z (Eq. (6)) v_{cr} is obtained from w for a known c_s .

Self-consistency of this method was carefully verified by several numerical investigations [18].

We use this method here for accurately assessing crack velocities.

3. Experimental assemblage

TerraTek tension machine (maximal axial stress up to 100 MPa; stiffness 5×10^9 N/m) was used for the measurement. It is operated by a closed-loop servocontrol (linearity 0.05%), which is used to maintain a constant axial piston rate of displacement. The axial load was measured with a load cell (linearity 0.5% full scale). An axial cantilever enables us to measure sample strain along the samples’ vertical axis. Each sample was uniaxially loaded by an axial displacement rate of 1 $\mu\text{m/s}$.

A magnetic one-loop antenna (EHFP-30 Near Field Probe set, Electro-Metrics Penril Corporation) 3 cm in diameter was

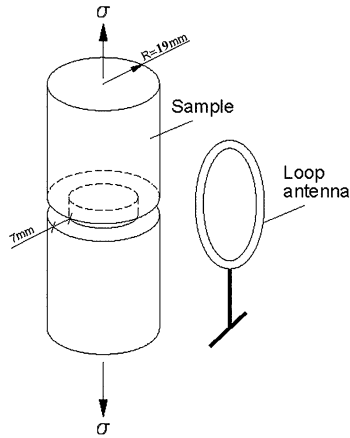


Fig. 1. The geometrical experimental setup. The cylinder of soda lime glass was pre-cut in the middle of its height normal to its vertical axis. The magnetic antenna is situated 2 cm away from the center of the samples with its normal pointing perpendicular to the cylinder axis.

used for the detection of the EMR. It is wound within a balanced Faraday shield, so that its response to external electric fields is vanishingly small. A low-noise micro-signal amplifier (Mitek Corporation Ltd., frequency range 10 kHz–500 MHz, gain 60 ± 0.5 dB, noise level 1.4 ± 0.1 dB throughout) and analog-to-digital converter connected to a triggered PC completed the detection equipment.

The antenna was situated 2 cm away from the center of the loaded samples with its normal pointing perpendicular to the cylinder axis (Fig. 1).

In this study cylindrical samples of soda-lime glass (10 cm in length and 3.8 cm in diameter) were used. The density of all investigated samples was 2600 kg/m^3 and the transverse acoustic wave velocity $c_s = 3330 \text{ m/s}$. The samples were pre-cut (at a depth of 7 mm) normal to their vertical axis in the middle of their length (Fig. 1) and hence the created tensile fracture occurred at the middle of the sample's length and in a sample of 24 mm in diameter.

4. Crack velocity calculation by both EMR and Wallner lines methods

Fig. 2 shows the crack surface created during the direct tension test. Wallner lines are clearly seen on more than 70% of the crack area.

The EMR signal induced by this fracture is shown in Fig. 3. It consists of numerous (partly overlapping) individual EMR pulses. Crack propagation velocity (Fig. 4) evaluated by the Wallner lines [18] was compared with the peak-amplitude of the EMR pulses (see Eqs. (1), (2)). To present the latter as a function of crack length, this length was calculated by integrating the $v(t)$ function of Fig. 3. The standard error of crack velocity calculation was between 6–21 m/s, that on average constitutes 0.65% of the measured crack velocity.

Both EMR peak amplitude and crack velocity calculated by Wallner lines analysis, v_w , fluctuate during crack propagation while their inter-correlation is obvious. Fig. 5 shows the re-

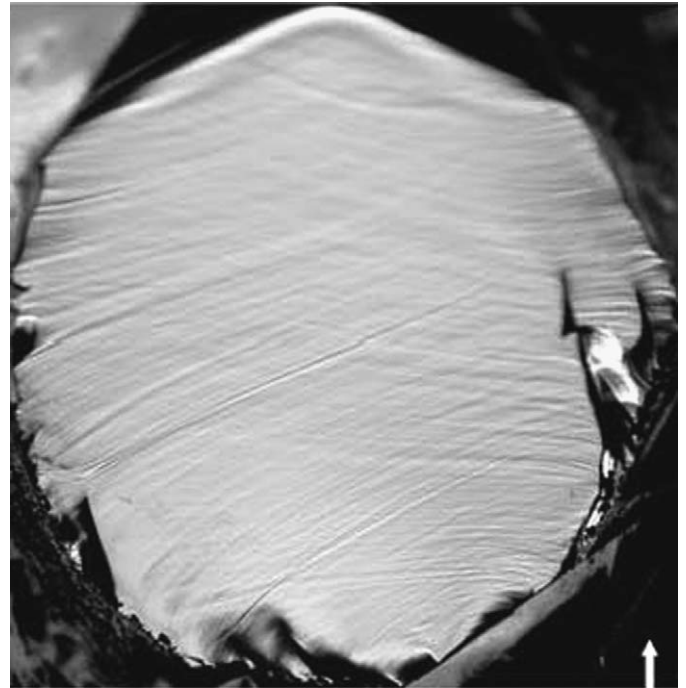


Fig. 2. Crack surface of fractured soda-lime glass sample loaded under direct tension. Many Wallner lines are visible. White arrow shows the direction of crack propagation.

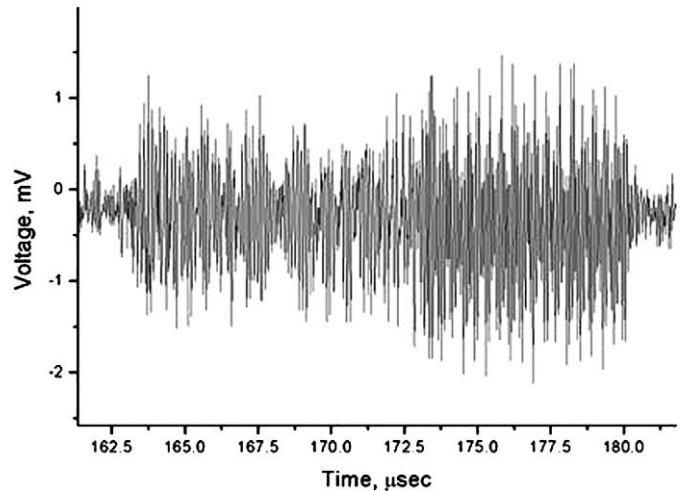


Fig. 3. EMR signal induced by the fracturing process of Fig. 2.

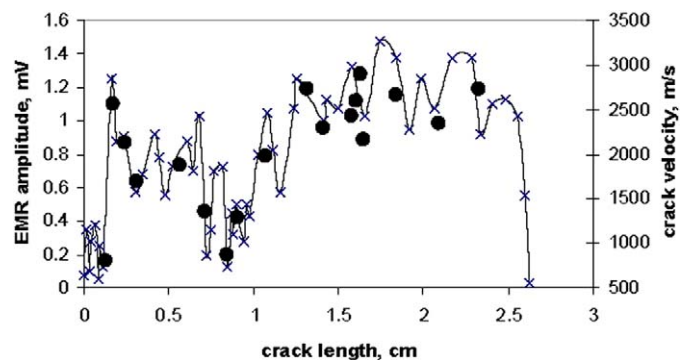


Fig. 4. A comparison between EMR amplitude (line with x's) and crack velocity (black circles), evaluated by the Wallner line method.

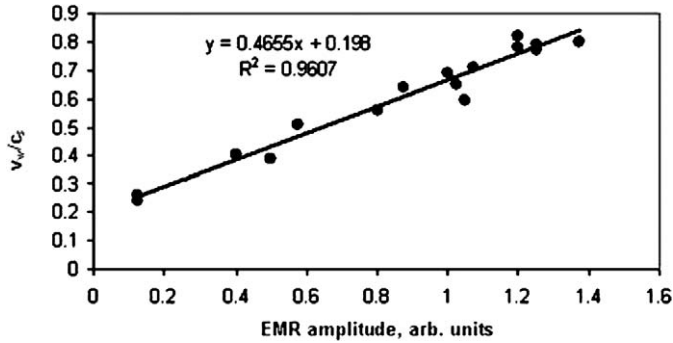


Fig. 5. Regression line between EMR pulse amplitude and crack velocity ratio (v_w/c_s , where c_s is the transverse wave velocity).

gression line between the EMR peak amplitude and the crack velocity ratio v_{cr}/c_s , yielding $R^2 = 0.96$.

The following data is needed to calculate the coefficient α_{glass} from Eq. (2): a value of the maximum amplitude of the EMR pulse A_0 , τ and the corresponding crack velocity v_{cr} . The latter is obtained by the Wallner lines method. Consider the value $A_0 = 1$ mV. According to Fig. 4 the corresponding crack velocity v_{cr} is 2209 m/s (calculated for $c_s = 3330$ m/s). Now, it was shown [19] that τ is a function of the pulse frequency ω and for glass can be obtained from

$$\tau = \frac{1.87}{(2\pi f)^{0.95}}. \quad (7)$$

The average EMR pulse frequency f (of pulses shown in Fig. 3) is 10.5 MHz, that yields (Eq. (7)) an estimate of τ to be 6.97×10^{-8} s. Eq. (2) then yields $\alpha_{\text{glass}} = 6495$.

5. Selfconsistency

Let us compare this coefficient with the one observed during our compressional loading of glass ceramics. We denote results of the glass ceramics experiments by the subscript gc. It was shown that the time to reach maximum amplitude, T , is related to the crack velocity [4,6,7] by

$$T = \frac{l}{v_{cr}}, \quad (8)$$

where l is crack length. Analysis of the fractured surface of glass ceramics [9] showed that the crack length was 93 mm while crack parameterization [9] yielded a value of $T_{gc} = 96 \mu\text{s}$, resulting in crack velocity $v_{cr_gc} = 968.75$ m/s. Pulse parameterization also yields $\tau_{gc} = 7.62 \times 10^{-5}$ s. Hence, by Eq. (2), $\alpha'_{gc} = 4.6$.

It follows from Eq. (3), that to compare this value to the one observed for glass, additional calibration factors must be taken into consideration. First, soda lime glass and glass ceramics are very similar brittle materials hence their values of EMR power, B , can be assumed to be equal. However the EMR

frequencies of the two experiments were different, the antenna responds differently to different signals frequencies of electromagnetic signals, and so do the signals amplifications.

The ratio of antenna response amplitudes is equal to the ratio of the respective frequencies [20]:

$$\frac{A_g}{A_{gc}} = \frac{\omega_g}{\omega_{gc}}, \quad (9)$$

where A_g and A_{gc} are the maximum pulse amplitudes while ω_g and ω_{gc} are the frequency for glass and glass ceramics, respectively. The averaged frequency of EMR signals observed during glass failure under tension was 6.6×10^7 while, ω_{gc} , during the glass ceramics test was 1.15×10^5 [9] yielding (Eq. (9)) an amplitude ratio of 574.

Signal amplification during the glass ceramics test was 60 dB while that during the glass test was 68 dB. Hence, the gain ratio is 2.5. The ratio α_{gc} for the same conditions as those for the glass experiment is obtained by a multiplication of these three factors, giving $\alpha_{gc} \approx 6630$, which is quite consistent with the $\alpha_{\text{glass}} \approx 6500$ obtained above for glass.

6. Conclusion

Our results indicate that the assumptions made are sound and the use of EMR peak amplitudes as a measure of relative crack velocities seems to be a valid procedure.

References

- [1] N. Khatishvili, Phys. Solid Earth 20 (1984) 656.
- [2] K. Fukui, S. Okubo, T. Terashima, Rock Mech. Rock Eng. (2005), in press.
- [3] Y.F. Contoyiannis, P.G. Kaporis, K.A. Eftaxias, Phys. Rev. E 71 (2005) 0661231.
- [4] A. Rabinovitch, V. Frid, D. Bahat, Philos. Mag. Lett. 77 (1998) 289.
- [5] A. Rabinovitch, V. Frid, D. Bahat, Philos. Mag. Lett. 79 (1999) 195.
- [6] D. Bahat, A. Rabinovitch, V. Frid, Tensile Fracture in Rocks, Springer, Heidelberg, 2005.
- [7] V. Frid, A. Rabinovitch, D. Bahat, J. Phys. D 36 (2003) 1620.
- [8] A. Rabinovitch, V. Frid, D. Bahat, J. Goldbaum, J. Appl. Phys. 93 (2003) 5085.
- [9] J. Goldbaum, V. Frid, D. Bahat, A. Rabinovitch, Meas. Sci. Technol. 14 (2003) 1839.
- [10] D. Bahat, Tectonofractography, Springer-Verlag, Berlin, 1991.
- [11] J.E. Field, Contemp. Phys. 12 (1971) 1.
- [12] H. Wallner, Z. Phys. 114 (1939) 368.
- [13] A. Smekal, Glastechn. Ber. 23 (1950) 57.
- [14] E.B. Shand, J. Am. Ceram. Soc. 37 (1954) 559.
- [15] E. Sharon, G. Cohen, J. Fineberg, Nature 410 (2001) 68.
- [16] D. Bonamy, K. Ravi-Chandr, Phys. Rev. Lett. 91 (2003) 2355021.
- [17] D. Hull, Fractography: Observing, Measuring and Interpreting Fracture Surface Topography, Cambridge Univ. Press, Cambridge, 1999.
- [18] A. Rabinovitch, V. Frid, D. Bahat, J. Appl. Phys. (2006), in press.
- [19] A. Rabinovitch, V. Frid, D. Bahat, J. Goldbaum, J. Appl. Phys. 93 (9) (2003) 5085.
- [20] A. Rabinovitch, V. Frid, D. Bahat, J. Goldbaum, Int. J. Rock Mech. Min. Sci. 37 (2000) 1149.